Available online at www.sciencedirect.com

SCIENCE DIRECT®

Earth and Planetary Science Letters 232 (2005) 393–402

EPSL

www.elsevier.com/locate/epsl

Solubility of rutile in subduction zone fluids, as determined by experiments in the hydrothermal diamond anvil cell

Andreas Audétat*, Hans Keppler[1]

Bayerisches Geoinstitut, Universität Bayreuth, 95440 Bayreuth, Germany

Received 8 August 2004; received in revised form 22 October 2004; accepted 14 January 2005
Available online 16 March 2005
Editor: B. Wood

Abstract

The solubility of rutile in H_2O (±NaCl, albite)-fluids was measured by direct observation of dissolving mineral grains within the hydrothermal diamond anvil cell. This new approach for studying mineral solubilities at high p/T has the advantage that the sample eventually gets completely dissolved and can be visually observed during this process, which eliminates the risk of overestimating true solubilities due to dissolution and reprecipitation during the run. Our measured rutile solubilities in pure H_2O are up to 1000 times lower than those reported in previous studies, ranging from 8 ppm to 26 ppm at 850–1000 °C/1.2–2.3 GPa. Nonlinear least square fitting of the data set resulted in the following equation for rutile solubility in pure water:

$$c_{TiO_2,fluid} = A\exp\left(\frac{-\Delta H^\circ}{RT}\right)\exp\left(\frac{-\Delta V^\circ}{RT}(p-1\ \text{bar})\right),$$

where A=8728.7 ppm, ΔH°=74,671 J·mol^{-1}, ΔV°=−0.61275 J·mol^{-1} K^{-1}, and p, T are given in bar and Kelvin, respectively. The presence of 9 wt.% dissolved albite leads to an increase in the TiO_2-solubility by a factor of 10, whereas addition of 15 wt.% NaCl results in a 2–3 times higher solubility than in pure water. Our results suggest that the solubility of TiO_2 (and, by inference, high field strength elements in general) in common mantle or subduction zone fluids is very low. In particular, the solubility of TiO_2 in these fluids is 2 to 3 orders of magnitude lower than the solubility of TiO_2 in clinopyroxene, implying a fluid/clinopyroxene partition coefficient of Ti in the order of 10^{-2} to 10^{-3}. This suggests that the presence of accessory phases such as rutile is not required to explain the high field strength element depletion in arc magmas.

Keywords: rutile; TiO_2; solubility; fluid; HDAC; diamond anvil cell; high field strength elements; HFSE; subduction zone

* Corresponding author. Tel.: +49 921 55 3713; fax: +49 921 55 3769.
E-mail addresses: andreas.audetat@uni-bayreuth.de (A. Audétat), hans.keppler@uni-bayreuth.de (H. Keppler).
[1] Tel.: +49 921 55 3744; fax: +49 921 55 3769.

0012-821X
doi:10.1016/j.epsl.2005.01.028

1. Introduction

Of the 10 most abundant components of silicate rocks, TiO_2 and Al_2O_3 are generally considered to be the least mobile ones. Titanium is therefore widely used as a reference element to recognize chemical changes associated with hydrothermal or metamorphic overprints [1]. Major host minerals of TiO_2 are rutile, titanomagnetite, sphene, and ilmenite, which frequently contain >90% of the whole-rock TiO_2-content. Rutile is among the most widespread of these minerals, occurring in rocks of plutonic, metamorphic as well as sedimentary origin. A special role has been attributed to rutile in subduction zone environments because it may be responsible for the characteristic depletion of high field strength elements (HFSE, e.g., Nb, Ta, Hf, Zr, Ti, V) relative to large ion lithophile elements (LILE, e.g., Rb, Sr, Cs, Ba, Th, U) in arc-related magmas [2].

Several hypotheses have been put forth to explain the origin of this feature, including: (1) relative immobility of HFSE during dehydration of the subducting slab [3–7], (2) preferential uptake of HFSE in the mantle wedge during the passage of slab-derived fluids or melts [8–10], (3) retention of HFSE during partial melting of the mantle [11], and (4) reaction of partial melts with mantle peridotite at later stages [12]. Of these models, the first one enjoys particular popularity because it seems to be supported by the largest number of natural and experimental evidence. It has been shown, for example, that rutile is frequently the dominant carrier of Nb and Ta in eclogites (often >90% of the whole-rock content; e.g., [7]), and that rutile/fluid partition coefficients of these two elements are extremely high (ranging from 6000 to 13,000 at 600 °C/1.0 GPa; [3]). Rutile – if present – therefore exerts a strong influence on fluid/rock partition coefficients of HFSE. The question whether rutile is present or not, is in turn a function of the TiO_2-solubility in the fluid. Precise knowledge of the solubility behavior of TiO_2 in high-P/T-fluids is therefore an important requisite to understand the HFSE-signature of arc-related magmas. Although it is unquestionable that rutile is a major sink for high field strength elements when it is present, it is not clear whether the depletion of high field strength elements can always be directly related to the presence of rutile in the subducted slab, as it is commonly assumed (e.g., [3,4,6]), or whether subduction zone fluids will be depleted in high field strength elements even if rutile is absent.

The first study on rutile solubility in fluids at mantle conditions was that of Ayers and Watson [13], who performed weight-loss experiments in piston-cylinders. For this purpose, they sealed previously weighed rutile single crystals together with aqueous solutions into platinum capsules and equilibrated them for 24 h at 800–1200 °C/1.0–2.9 GPa. After quenching, the crystals were re-weighed, and TiO_2-solubilities were calculated on the basis of the difference to the starting weight. Although problems with rutile redistribution due to temperature gradients were noticed, the calculated maximum solubilities of 0.15 wt.% to 1.9 wt.% TiO_2 were considered to be representative. Recently, Tropper and Manning [14,15] repeated these experiments using the same technique, but with a more rigorous control on temperature gradients and a more discriminating interpretation of newly formed rutile crystals. By using an inner Pt-envelope, they were able to significantly reduce temperature gradients along the charge, which resulted in less TiO_2-redistribution during the run. Their calculated TiO_2-solubilities are up to 80 times lower than those obtained by [13]. In the present study, we followed a completely new approach by dissolving tiny pieces of rutile in a hydrothermal diamond anvil cell (HDAC). This technique has the advantage that the sample can be visually observed during the run, which ultimately leads to much less ambiguity in the interpretation of the results.

2. Methods

Experiments were performed in an externally-heated hydrothermal diamond anvil cell of the Bassett-type [16,17]. In this apparatus, the sample is contained in the borehole of a small metal gasket that is compressed between two diamond anvils. The resulting sample chamber is confined at the bottom and the top by the two diamond anvils, and on the side by the metal gasket. For our experiments, we used gaskets made of rhenium or iridium, with boreholes measuring 500 μm in diameter. Both diamonds anvils

can be heated independently by molybdenum wire resistance heaters to a maximum temperature of ca. 1100 °C. Pressure is mostly generated during heating because the filling medium (usually H_2O) is confined in a chamber of ± fixed volume [18]. The chamber content therefore follows an approximately isochoric path defined by its bulk density. The basic idea behind our solubility measurements is very simple: a specific amount of rutile is loaded together with a known amount of water into the sample chamber, and subsequently heated up until all rutile is dissolved. The temperature at which the last grain of rutile disappears marks the solubility of the loaded amount of rutile at the particular P/T-condition reached at this point (Fig. 1). By varying the water density and the amount of added rutile, different TiO_2-solubilites can be obtained at different P/T-conditions, which results in a number of data points through which isopleths can be fitted. As will be shown below, the main difficulty of this technique lies in the precise measure-

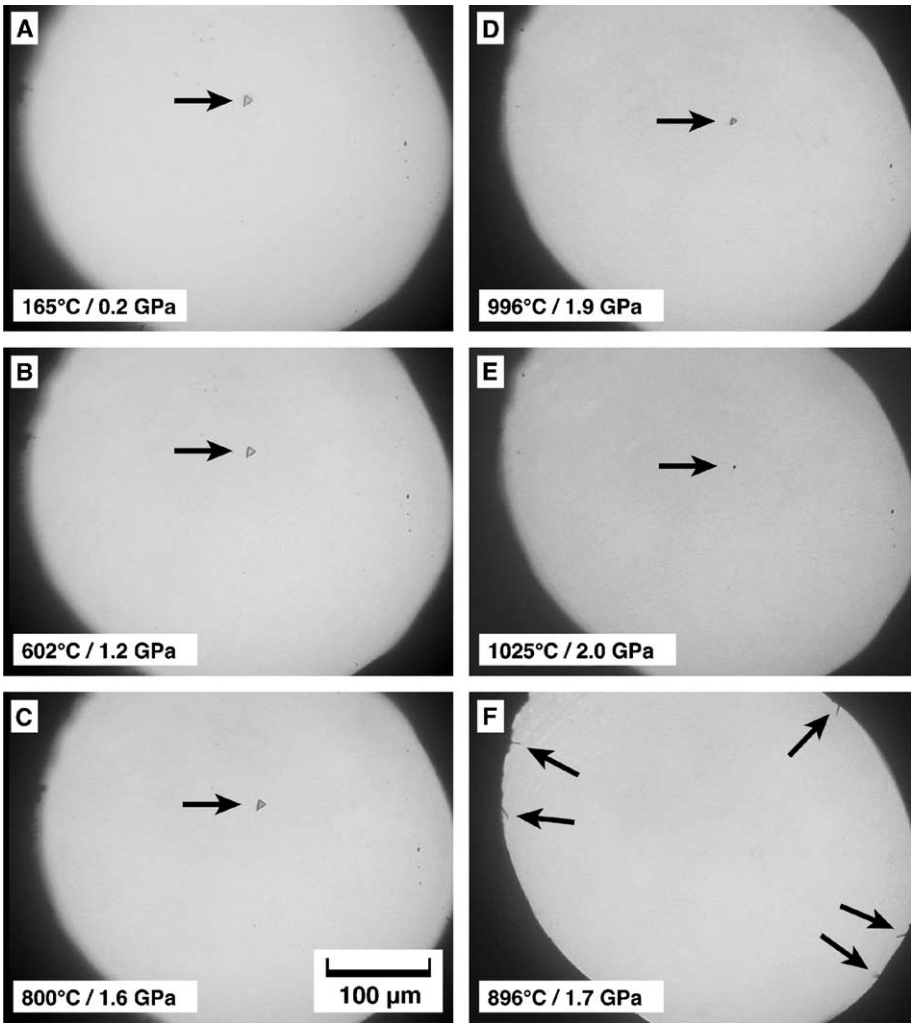

Fig. 1. Run sequence of the dissolution of a piece of rutile in pure H_2O. (A) View of the sample chamber at 165 °C/0.2 GPa. The arrow points to the piece of rutile, which measures 11.0 µm in the longest dimension. (B–C) The size of the rutile piece remains unchanged during heating to 602 °C/1.2 GPa and 800 °C/1.6 GPa, respectively. (D) At 996 °C/1.9 GPa, a significant portion of rutile is dissolved in the surrounding fluid. (E) Disappearance of the last grain of rutile at 1025 °C/2.0 GPa. (F) Cooling to 896 °C/1.7 GPa results in the precipitation of thin rutile needles at different sites along the Re-gasket.

ment (and handling) of the pieces of rutile loaded into the sample chamber.

Tiny pieces of rutile with measurable volume were prepared from a single, gem quality rutile crystal from Brazil by manufacturing a doubly-polished section of 2.0–8.0 μm thickness, and subsequently breaking it into geometric pieces. The exact thickness of each piece was calculated from its interference color relative to that of the thickest part of the section, which was measured in the microscope at 8.0 ± 0.5 μm. Due to the extremely high birefringence of rutile (leading to rapid color changes with increasing thickness), this method allows measurement of the width of a 2.0 μm-thick rutile piece with an uncertainty of 0.1 μm. The uncertainty in the measurement of the other two dimensions was fixed by the optical resolution of the microscope at 0.5 μm. Although small on an absolute basis, these uncertainties sum up to ±20% relative for a piece measuring 10.0×5.0×2.0 μm, which corresponds to the average size of rutile pieces used in this study.

After loading the rutile, the rest of the sample chamber was filled with distilled water, whereby a vapor bubble was left to constrain the starting density. The mass of added water was calculated from its bulk density (derived from the liquid-vapor homogenization temperature) and the volume of the sample chamber. Because the sample chamber commonly was distorted due to pre-runs performed with pure H_2O to get a tight seal, its volume could not easily be calculated by geometric means. Instead, the chamber volume was calculated from the size of the vapor bubble at a given temperature, the corresponding densities of liquid and vapor, and the total density (ρ_{tot}) of the water filled into the chamber according to the formula:

$$\mathrm{Vol}_{cell} = \frac{\mathrm{Vol}_{vap}(\rho - \rho_{liq})}{(\rho_{tot} - \rho_{liq})}. \quad (1)$$

By measuring the size of the vapor bubble at different temperatures, five independent calculations of the sample chamber volume were obtained for each experiment. The results usually were reproducible within ±2–4% relative. Overall uncertainties in the weight fraction of rutile loaded into the sample chamber therefore ranged from 20% to 30% relative, depending on the geometry and size of the rutile piece, and the reproducibility of the chamber volume determination.

After loading, the sample chamber was heated with a rate of 30–40 °C/min until the first signs of rutile dissolution appeared (this usually happened around 700–750 °C). The heating rate was then lowered to 10–20 °C/min in order to allow enough time for temporal equilibration between rutile and the surrounding fluid. The following observations suggest that temporal equilibrium indeed was attained: (i) if the temperature was held constant, the size of the crystal did not change, (ii) if the temperature was lowered *before* complete dissolution occurred, the crystal immediately started to grow again, and (iii) if the temperature was lowered *after* complete dissolution occurred, thin rutile needles precipitated along the walls of the sample chamber. In the latter case, however, rutile precipitation did not start until the temperature was lowered 20–50 °C below the homogenization temperature. This behavior is probably a result of supersaturation.

An order-of-magnitude estimation of the time required to reach equilibrium in our experiments can be made as follows. The diffusion coefficient of Ti in aqueous fluids at high P/T is not known. However, since Ti^{4+} most likely dissolves in the fluid as some kind of hydrated species, the diffusion coefficient of Ti^{4+} is probably within one or two orders of magnitude of the diffusion coefficient of H_2O. The latter can be estimated from the viscosity (at the P/T-conditions of interest) according to Eyring's equation:

$$D = \frac{kT}{\eta\lambda}, \quad (2)$$

where D is the diffusion coefficient, k is the Boltzmann constant, T the temperature (in Kelvin), η the viscosity, and λ the mean distance between the water molecules. At 800 °C/2.0 GPa (i.e., at the low-temperature, high-density end of our data set), the viscosity of water is estimated from [19] to be in the order of 6×10^{-5} Pa·s, whereas the average distance between water molecules (calculated from the fluid density) is 3.1 Å. With these values, a diffusion coefficient of 8.0×10^{-7} m^2 s^{-1} is returned. The time required for a particle to diffuse over the distance χ is related to the diffusion coefficient D by:

$$t = \frac{\chi^2}{2D}. \quad (3)$$

Hence, at 800 °C/2.0 GPa, in the order of 0.16 s are needed for a titanium complex to travel across the

entire sample chamber (500 μm diameter). This result is in accord with our observation that the dissolution behavior responses fast to changes in temperature.

Apart from solubility measurements in pure H_2O, we also conducted experiments in aqueous solutions containing 15 wt.% NaCl or 9 wt.% albite. Albite was added in the form of geometric pieces of albite glass, the volume of which was determined in a manner similar to the one described above. In both runs with albite, the albite glass dissolved ca. 200 °C below the dissolution temperature of rutile.

In order to avoid TiO_2-contamination from earlier runs, we always used a new metal gasket for each solubility measurement. Oxygen fugacity was not strictly buffered in our experiments. It is probable that in the experiments with rhenium gaskets the oxygen fugacity was buffered close to Re/ReO_2 due to a thin surface film of rhenium oxide on the gasket surface. In any case, changes in oxygen fugacity are not considered to be important in these experiments, since Ti^{4+} is the only stable oxidation state of titanium over a wide range of redox conditions.

Temperatures of final rutile dissolution were recorded by Ni–Cr-thermocouples that were calibrated against the melting points of $NaNO_3$, CsCl, and NaCl observed inside the sample chamber at ambient pressure. Associated uncertainties are in the order of 5–10 °C in the temperature range of 800–1000 °C. Pressures at the time of final rutile dissolution were calculated from the fluid density after cooling, using equations of state for H_2O [20] and H_2O–NaCl solutions [21–24] in the case of NaCl-bearing experiments. For the albite-bearing runs, it was assumed that the dissolution of albite glass is accompanied by zero excess volume of mixing. If no vapor bubble was present after cooling to room temperature, fluid densities were calculated from the melting point of ice using the formulas described in [25,26]. Overall uncertainties in the pressure determination are estimated to be ≤0.06 GPa for experiments with pure H_2O, and ≤0.16 GPa in the case of NaCl-bearing runs (the latter resulting from large extrapolations).

3. Results

Experimental results are plotted in Fig. 2 and listed in Table 1. Solubility measurements in pure H_2O were conducted in both Re-gaskets and Ir-gaskets. Values obtained from runs with pure water using Re-gaskets range from 8 ppm to 26 ppm, and increase regularly with increasing pressure and temperature (black dots in Fig. 2). Two control measurements performed in Ir-gaskets (white dots in Fig. 2), however, returned somewhat higher values. Potential explanations for this discrepancy are: (i) alloying of Ti with the Ir-gasket, (ii) adsorption of a titanium compound as a thin layer along the Ir-gasket wall, or (iii) dissolution of traces of Re leading to changes in the solvent pH that may affect rutile solubility. Because two of these possibilities result in artificially high values, we consider the values obtained from Re-gaskets as more reliable. The corresponding 10 data points were then used to derive an equation that yields TiO_2-solubility in pure H_2O as a function of pressure and temperature. TiO_2-dissolution in pure water can be described by:

$$TiO_{2\ (s)} \rightarrow TiO_{2\ (aq)} \tag{4}$$

The equilibrium constant (K) of this reaction is equal to the activity of TiO_2 in the fluid, and is related to temperature and pressure by

$$-RT\ln K = \Delta H^\circ - T\Delta S^\circ + \Delta V^\circ(p-1), \tag{5}$$

where R is the gas constant (8.314 $J\cdot mol^{-1}\cdot K^{-1}$), T the temperature (in K), p the pressure (in bar), ΔH° the change in enthalpy, ΔS° the change in entropy, and ΔV° the change in molar volume upon dissolution of rutile. Solution for K leads to:

$$K = a_{TiO_2,\mathrm{fluid}} = \exp\left(\frac{\Delta S^\circ}{R}\right)\exp\left(\frac{-\Delta H^\circ}{RT}\right)\exp\left(\frac{-\Delta V^\circ}{RT}(p-1)\right) \tag{6}$$

If the activity coefficient of TiO_2 in the fluid is constant over the p, T, and concentration range studied, the concentration of TiO_2 in the fluid is directly proportional to K. With this assumption, Eq. (6) can be rearranged to:

$$c_{TiO_2,\mathrm{fluid}} = A\exp\left(\frac{-\Delta H^\circ}{RT}\right)\exp\left(\frac{-\Delta V^\circ}{RT}(p-1\ \mathrm{bar})\right). \tag{7}$$

Nonlinear least square fitting of an equation of this type through our 10 data points returned the following

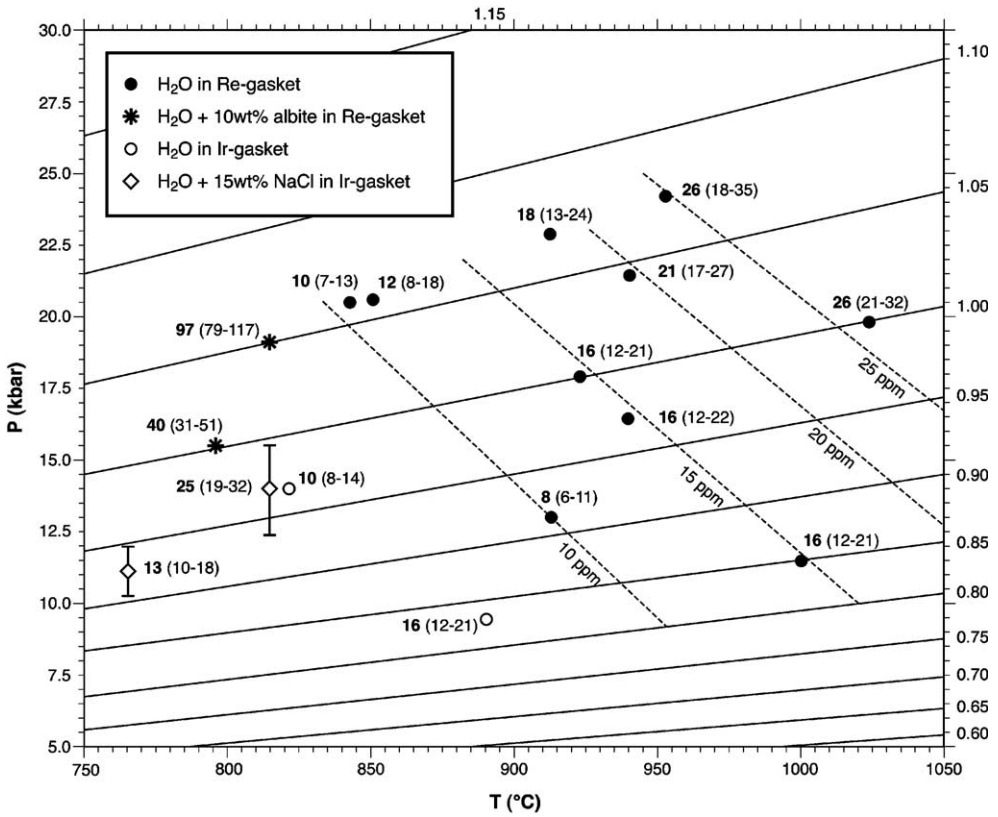

Fig. 2. P/T-diagram showing all solubility data obtained during this study. The numbers next to each symbol denote the calculated mass of loaded rutile (in ppm), with the uncertainty range shown in parentheses. Also included are isochores of H_2O (full lines; densities given in g/cm^3 on the right) and isopleths of TiO_2-solubilites in pure water (dashed lines) calculated from Eq. (7) in the text.

values: A=8728,7 ppm; ΔH°=74,671 J·mol^{-1}, and ΔV°=−0.61275 J mol^{-1} K^{-1}, with an associated statistical uncertainty of χ^2=1.99. This equation was used to calculate the solubility curves of 10, 15, 20, and 25 ppm TiO_2 shown in Fig. 2.

Experiments with added NaCl were performed in Ir-gaskets because we observed corrosion of the rhenium gasket in contact with Cl-bearing solutions at high temperature. Comparison of the two data points from Cl-bearing runs (gray diamonds in Fig. 2) with those from Cl-free runs in Ir-gaskets (white dots in Fig. 2) suggests that the solubility of TiO_2 in a 15 wt.% NaCl solution is about 2–3 times higher than that in pure H_2O.

Experiments with added albite were conducted in Re-gaskets. Unfortunately, they were hampered by the formation of an unidentified mineral at temperatures above 800–850 °C, which crystallized in the form of hexagonal platelets resembling mica. Because this mineral grew at the expense of rutile (suggesting that it incorporates TiO_2), we discarded all experiments in which the mineral started to crystallize before the rutile crystal was completely dissolved. The remaining two data points (stars in Fig. 2) suggest that the addition of 9 wt.% albite leads to an approximately 10-fold increase in TiO_2-solubility compared to that in pure water.

4. Discussion

4.1. Rutile solubility and experimental strategies for solubility measurements in fluids at high p and T

Our measured TiO_2-solubilities in H_2O are three orders of magnitude lower than those reported by

Table 1
Experimental rutile solubility data

Rutile (ppm)[a]	X_{rutile}[b]	$T_{dissol.}$ (°C)	$P_{dissol.}$ (GPa)	Gasket	Fluid
12 (8–18)	2.71E-06	850 ± 9	2.06 ± 0.05	Re	H_2O
16 (12–22)	3.61E-06	940 ± 9	1.65 ± 0.04	Re	H_2O
10 (7–13)	2.26E-06	843 ± 8	2.05 ± 0.05	Re	H_2O
24 (18–31)	5.41E-06	948 ± 9	1.98 ± 0.05	Re	H_2O
26 (21–32)	5.86E-06	1025 ± 10	1.99 ± 0.05	Re	H_2O
18 (13–24)	4.06E-06	912 ± 9	2.29 ± 0.06	Re	H_2O
8 (6–11)	1.80E-06	912 ± 9	1.29 ± 0.03	Re	H_2O
16 (12–21)	3.61E-06	1000 ± 10	1.15 ± 0.03	Re	H_2O
16 (12–21)	3.61E-06	923 ± 9	1.79 ± 0.04	Re	H_2O
21 (17–27)	4.74E-06	941 ± 9	2.15 ± 0.05	Re	H_2O
10 (6–14)	2.26E-06	821 ± 8	1.40 ± 0.04	Ir	H_2O
16 (12–21)	3.61E-06	891 ± 9	0.95 ± 0.02	Ir	H_2O
13 (10–18)	2.93E-06	764 ± 8	1.11 ± 0.08	Ir	15 wt.% NaCl
25 (19–32)	5.64E-06	814 ± 8	1.40 ± 0.16	Ir	15 wt.% NaCl
96 (79–117)	2.17E–05	815 ± 8	1.21 ± 0.03	Re	9.4 (7.3–11.5) wt.% albite
40 (31–51)	9.02E-06	796 ± 8	1.54 ± 0.04	Re	8.8 (7.7–10.1) wt.% albite

[a] Uncertainty range shown in parentheses.
[b] Mole fraction.

[13], and between 6 and 10 times lower than those reported by [14,15]. We believe that all these earlier data are too high due to substantial mobilization and reprecipitation of TiO_2 during the experiments. Apparently, even in the arrangement of Tropper and Manning [14,15] (i.e., using a thick-walled graphite furnace, an inner Pt-envelope, and a short, horizontal Pt-capsule), temperature gradients cold not be minimized enough to prevent TiO_2-mobilization. If this interpretation is correct, it implies that weight-loss experiments are notoriously difficult to interpret and may frequently result in an overestimation of the true solubility. Because our approach is based on *complete* dissolution (with a visual control of this process), there is no danger of overestimating solubilities unless the sample reacts with the metal gasket. Solubilities can be underestimated, however, if the sample is heated too rapidly. As was shown above, this can be avoided by performing a few simple tests.

The large overestimation of rutile solubility in the experiments of Ayers and Watson [13] demonstrates impressively that even very insoluble substances can be transported in significant quantities and in short time-scales as a result of small gradients in temperature (and, by inference, in pressure). The common presence of rutile crystals in eclogitic veins and alpine-type fissure-veins, which has been regarded as evidence for high TiO_2-solubilities in the respon-

sible fluids, could therefore simply be the result of fluid circulation. Field evidence for extensive precipitation of hydrothermal minerals should not be generally attributed to high solubilities. Massive gold mineralization, for example, typically forms from fluids that carry a few ppm Au at most. As demonstrated by the previous experimental studies on rutile solubility, significant mass transport can occur in a fluid system even if both the solubility and temperature gradients are low. Efficient mass transport in such a situation is possible if the enthalpy of dissolution is high (leading to a strong temperature dependence of solubility), and if the nucleation barrier for the mineral of interest is low. In nature, mass transport may further be aided by gradients in chemical potential and large-scale fluid circulation.

The fact that the TiO_2-solubility in a 15 wt.% NaCl-solution is enhanced relative to that in pure water is probably not a consequence of Cl-complexing. More likely, it is a result of the higher ionic strength of the solution, or it may be due to the stabilization of hydroxy complexes due to changes in pH. The elevated TiO_2-solubility in the presence of 9 wt.% albite is explained by the fact that TiO_2-solubilities in silicate melts are comparatively high. For example, rutile saturation in an evolved granitic melt at 1000 °C/2.0 GPa is attained at 1.5 wt.% TiO_2 [27], and in an albitic or granitic melt around 800 °C

at ca. 0.3 wt.% TiO_2 [28,29]. A simple "mechanical" mixture of 90% H_2O and 9 wt.% albite melt, each saturated with rutile at 800 °C/2.0 GPa would therefore result in a TiO_2-solubility of about 270 ppm, which is reasonably close to the actually measured value of 97 ppm.

It should be noted that the fluid compositions used in our experiments – although a valid approximate for many natural fluids – are rather simple. Rutile solubility may increase in the presence of fluorine or in strongly alkaline solutions due to the high solubility of fluoride and hydroxy complexes of Ti^{4+}. Rutile and elemental titanium are known to be soluble in hydrofluoric acid, and the formation of $Ti(OH)_4F_2^{2-}$ and $Ti(OH)_2F_4^{2-}$ complexes was suggested by [30]. Reports of rutile and ilmenite daughter phases in fluid inclusions from eclogite-facies rocks [31] may be interpreted as evidence for the existence of unusual titanium-rich fluids in nature.

4.2. The origin of the high field strength element depletion in subduction zone magmas

The characteristic depletion of HFSE elements in arc magmas is usually attributed to the depletion of these elements in the hydrous fluids released from the subducted slab. In equilibrium with an aqueous fluid, these elements strongly partition into rutile, and since rutile is a common accessory mineral in eclogites, the HFSE depletion is often simply explained as the result of the presence of rutile in the subducted slab. While it is unquestionable that the presence of rutile does indeed deplete a fluid in high field strength elements, we will demonstrate here that rutile is neither required for this depletion to develop, nor can the presence of rutile in the subducted slab alone explain the trace element pattern observed in arc magmas.

The solubility of TiO_2 in $CaMgSi_2O_6$ diopside is in the order of 1–2 wt.% and increases strongly with the aluminum content of the clinopyroxene due to the coupled substitution of $Ti^{4+}Al_2^{3+}$ for $Mg^{2+}Si_2^{4+}$ [32]. Since according to our study the solubility of TiO_2 in aqueous fluids of a range of compositions is in the order of 10 to 100 ppm only, the fluid/clinopyroxene partition coefficient of titanium, $D_{Ti}^{fluid/cpx}$, is in the order of 10^{-2} to 10^{-3}, roughly consistent with previous estimates by [5]. Therefore, titanium would be removed from a subduction zone fluid by exchange with clinopyroxene, even if no rutile were present. More importantly, during percolation of this fluid through the mantle wedge above the subducted slab, chemical exchange between the fluid and the mantle peridotite will not lead to an enrichment of the fluid with titanium. This is essential for the HFSE depletion of the fluid to be preserved until the fluid enters the zone of melting. Since mantle peridotite generally does not contain rutile or other accessory phases that concentrate HFSE elements, this is only possible if titanium partitions in favour of some major silicate phase in equilibrium with an aqueous fluid. Even if rutile played a major role in depleting the fluid in titanium when is it generated by dehydration reactions inside the subducted slab, this depletion would disappear during percolation of the fluid through the mantle wedge if the solubility of TiO_2 in the fluid was not intrinsically lower than the TiO_2 solubility in clinopyroxene, leading to a preferential partitioning of TiO_2 in favour of the pyroxene phase. Simple statements such as "the HFSE depletion in arc magmas is due to the presence of rutile in the subducted slab" are therefore misleading. In reality, the HFSE depletion is due to the intrinsically low solubility of these elements in hydrous fluids, which causes them to become enriched in accessory phases and/or clinopyroxene.

5. Conclusions

This study demonstrates that mineral solubilities down to the ppm-level can be measured by direct observation of dissolving mineral grains in the diamond anvil cell. A major advantage of this technique lies in the fact that the sample is completely dissolved and can be visually observed during this process, which results in much less ambiguity in the interpretation of the results compared to the weight-loss method. Our measured rutile solubilities in pure H_2O are up to three orders of magnitude lower than previously published values, reaching no more than 30 ppm at 1000 °C/2.0 GPa. We believe that the results obtained in these earlier studies are too high due to TiO_2-redistribution during the experiments. Fitting a thermodynamically founded equation through our data points results in

the following equation for TiO_2-solubility in H_2O (T in K; p in bar):

$$c_{TiO_2,\mathrm{fluid}} = A\exp\left(\frac{-\Delta H^\circ}{RT}\right)\exp\left(\frac{-\Delta V^\circ}{RT}(p-1\ \mathrm{bar})\right), \quad (7)$$

with $A=8728.7$ ppm, $\Delta H^\circ = 74{,}671\ \mathrm{J\cdot mol^{-1}}$, and $\Delta V^\circ = -0.61275\ \mathrm{J\cdot mol^{-1}\cdot K^{-1}}$.

According to our experiments, TiO_2-solubility in aqueous solutions with 15 wt.% NaCl is about 2–3 times higher than in pure water, whereas the presence of 9 wt.% dissolved albite causes an increase in TiO_2-solubility by about one order of magnitude. In general, however, rutile solubilities observed in this study are rather low (<100 ppm), which justifies the common use of Ti as a reference element for monitoring chemical differences between altered and unaltered rocks. Because HFSE behave chemically similar, it is expected that V, Hf, Zr, Nb, and Ta show similarly low solubilities in $H_2O \pm NaCl \pm$ albite-fluids. If this is correct, the characteristic depletion of HFSE relative to LILE in arc-related magmas can in principle be achieved also without the presence of residual rutile, because LILE are generally more soluble than HFSE [5]. If residual rutile or other HFSE-rich phases are present, however, the HFSE/LILE-ratio of fluids equilibrated with such rocks will be strongly controlled by these minerals. It should be noted that these conclusions hold only for fluid compositions in the systems H_2O–NaCl and H_2O–albite. Addition of other components such as fluorine may result in significantly higher TiO_2-solubilities.

Acknowledgements

Very constructive reviews by Bruce Watson and Craig Manning are gratefully acknowledged. This study was supported by the German Science Foundation (DFG; Leibniz award to HK).

References

[1] H. Rollinson, Using Geochemical Data: Evaluation, Presentation, Interpretation, Longman, 1993, 352 pp.
[2] Y. Tatsumi, S. Eggins, Subduction Zone Magmatism, Blackwell, Cambridge, 1995, 211 pp.
[3] J.M. Brenan, H.F. Shaw, D.L. Phinney, F.J. Ryerson, Rutile-aqueous fluid partitioning of Nb, Ta, Hf, Zr, U and Th: implications for high field strength element depletions in island-arc basalts, Earth Planet. Sci. Lett. 128 (1994) 327–339.
[4] J.M. Brenan, H.F. Shaw, F.J. Ryerson, D.L. Phinney, Mineral-aqueous fluid partitioning of trace elements at 900 °C and 2.0 GPa: constraints on the trace element chemistry of mantle and deep crustal fluids, Geochim. Cosmochim. Acta 59 (1995) 3331–3350.
[5] H. Keppler, Constraints from partitioning experiments on the composition of subduction-zone fluids, Nature 380 (1996) 237–240.
[6] R. Stalder, S.F. Foley, G.P. Brey, I. Horn, Mineral-aqueous fluid partitioning of trace elements at 900–1200 °C and 3.05.7 GPa: new experimental data for garnet, clinopyroxene and rutile, and implications for mantle metasomatism, Geochim. Cosmochim. Acta 62 (1998) 1781–1801.
[7] T. Zack, A. Kronz, S.F. Foley, T. Rivers, Trace element abundances in rutiles from eclogites and associated garnet mica schists, Chem. Geol. 184 (2002) 97–122.
[8] D.A. Ionov, A.W. Hofmann, Nb–Ta-rich mantle amphiboles and micas: implications for subduction-related metasomatic trace element fractionations, Earth Planet. Sci. Lett. 131 (1995) 341–356.
[9] J. Ayers, Trace element modeling of aqueous fluid–peridotite interaction in the mantle wedge of subduction zones, Contrib. Mineral. Petrol. 132 (1998) 390–404.
[10] F. Kalfoun, D. Ionov, C. Merlet, HFSE residence and Nb/Ta ratios in metasomatised, rutile-bearing mantle peridotites, Earth Planet. Sci. Lett. 199 (2002) 49–65.
[11] A.D. Saunders, J. Tarney, S.D. Weaver, Transverse geochemical variations across the Antarctic peninsula: implications for the genesis of calc-alkaline magmas, Earth Planet. Sci. Lett. 46 (1980) 344–360.
[12] P.B. Kelemen, N. Shimizu, T. Dunn, Relative depletion of niobium in some arc magmas and the continental crust: partitioning of K, Nb, La and Ce during melt/rock reaction in the upper mantle, Earth Planet. Sci. Lett. 120 (1993) 111–134.
[13] J.C. Ayers, E.B. Watson, Rutile solubility and mobility in supercritical aqueous fluids, Contrib. Mineral. Petrol. 114 (1993) 321–330.
[14] P. Tropper, C.E. Manning, Very low solubility of rutile in H_2O at high p and T, Eos. Trans. AGU, Fall Meet. Suppl. 84 (2003) (abstract V22D-0611).
[15] P. Tropper, C.E. Manning, The solubility of rutile and corundum in H_2O at high P and T: constraints on Ti and Al-mobility during high-P metamorphism, EMPG-X, Symposium abstracts, Lithos 73 (2004) S113.
[16] W.A. Bassett, A.H. Shen, M. Buckum, A new diamond anvil cell for hydrothermal studies to 2.5 GPa and from −190 °C to 1200 °C, Rev. Sci. Instrum. 64 (1993) 2340–2345.
[17] W.A. Bassett, A.H. Shen, M. Buckum, I.M. Chou, Hydrothermal studies in a new diamond anvil cell up to 10 GPa and from −190 °C to 1200 °C, Pure Appl. Geophys. 141 (1993) 487–495.
[18] A.H. Shen, W.A. Bassett, I.M. Chou, Hydrothermal studies in a diamond anvil cell: pressure determination using the

equation of state, in: Y. Syono, M.H. Manghnani (Eds.), High-pressure Research: Application to Earth and Planetary Sciences, American Geophysical Union, Washington, 1992, pp. 61–68.
[19] IAPWS, Revised release on the IAPS Formulation 1985 for the Viscosity of Ordinary Water Substance, Erlangen, Germany, 1997.
[20] A. Saul, W. Wagner, A fundamental equation for water covering the range from the melting line to 1273 K at pressures up to 25,000 MPa, J. Phys. Chem. Ref. Data 18 (1989) 1537–1564.
[21] T.S. Bowers, H.C. Helgeson, Calculation of the thermodynamic and geochemical consequences of nonideal mixing in the system H_2O–CO_2–NaCl on phase relations in geologic systems: equation of state for H_2O–CO_2–NaCl fluids at high pressures and temperatures, Geochim. Cosmochim. Acta 47 (1983) 1247–1275.
[22] P.E. Brown, W.M. Lamb, PVT properties of fluids in the system H_2OCO_2NaCl: new graphical presentations and implications for fluid inclusion studies, Geochim. Cosmochim. Acta 53 (1989) 1209–1221.
[23] A. Anderko, K.S. Pitzer, Equation-of-state representation of phase equilibria and volumetric properties of the system NaCl–H_2O above 573K, Geochim. Cosmochim. Acta 57 (1993) 1657–1680.
[24] R.J. Bodnar, M.O. Vityk, Interpretation of microthermometric data for H_2O–NaCl fluid inclusions, in: B.D. Vivo, M.L. Frezzotti (Eds.), Fluid Inclusions in Minerals: Methods and Applications, Virginia Tech, Blacksburg, VA, USA, 1994, pp. 117–130.
[25] W. Wagner, A. Saul, A. Pruss, International equations for the pressure along the melting and along the sublimation curve of ordinary water substance, J. Phys. Chem. Ref. Data 23 (1994) 515–525.
[26] H. Tanaka, Simple physical model of liquid water, J. Chem. Phys. 112 (2000) 799–809.
[27] T.H. Green, J. Adam, Pressure effect on Ti- or P-rich accessory mineral saturation in evolved granitic melts with differing K_2O/Na_2O-ratios, Lithos 61 (2002) 271–282.
[28] F.J. Ryerson, E.B. Watson, Rutile saturation in magmas: implications for Ti–Nb–Ta depletion in island-arc basalts, Earth Planet. Sci. Lett. 86 (1987) 225–239.
[29] H. Keppler, Influence of fluorine on the enrichment of high field strength trace elements in granitic rocks, Contrib. Mineral. Petrol. 114 (1993) 479–488.
[30] K.H. Barsukova, V.A. Kuznetov, V.A. Dorofeyeva, L.I. Khodakovskiy, Measurement of the solubility of rutile TiO_2 in fluoride solutions at elevated temperatures, Geokhimiya 7 (1979) 1017–1027.
[31] P. Philippot, J. Selverstone, Trace-element-rich brines in eclogitic veins: implications for fluid composition and transport during subduction, Contrib. Mineral. Petrol. 106 (1991) 417–430.
[32] B. Sepp, T. Kunzmann, The stability of clinopyroxene in the system CaO–MgO–SiO_2–TiO_2 (CMST), Am. Mineral. 86 (2001) 265–270.